

Nonlinear Seebeck and Peltier effects in a Majorana nanowire coupled to leads

Feng Chi(迟锋), Jia Liu(刘佳), Zhenguo Fu(付振国), Liming Liu(刘黎明), and Zichuan Yi(易子川)

Citation: Chin. Phys. B, 2024, 33 (**7**): 077301. DOI: 10.1088/1674-1056/ad3f99
Journal homepage: http://cpb.iphy.ac.cn; http://iopscience.iop.org/cpb

What follows is a list of articles you may be interested in

Manipulation of internal blockage in triangular triple quantum dot

Yue Qi(齐月) and Jian-Hua Wei(魏建华)
Chin. Phys. B, 2024, 33 (**5**): 057301. DOI: 10.1088/1674-1056/ad2d54

Chiral current regulation and detection of Berry phase in triangular triple quantum dots

Yue Qi(齐月), Yi-Ming Liu(刘一铭), Yuan-Dong Wang(王援东), Jian-Hua Wei(魏建华), and Zhen-Gang Zhu(朱振刚)
Chin. Phys. B, 2023, 32 (**8**): 087304. DOI: 10.1088/1674-1056/acd36c

Coherent manipulation of a tunable hybrid qubit via microwave control

Si-Si Gu(顾思思), Bao-Chuan Wang(王保传), Hai-Ou Li(李海欧), Gang Cao(曹刚), and Guo-Ping Guo(郭国平)
Chin. Phys. B, 2023, 32 (**8**): 087302. DOI: 10.1088/1674-1056/acd0a7

Delayed response to the photovoltaic performance in a double quantum dots photocell with spatially correlated fluctuation

Sheng-Nan Zhu(祝胜男), Shun-Cai Zhao(赵顺才), Lu-Xin Xu(许路昕), and Lin-Jie Chen(陈林杰)
Chin. Phys. B, 2023, 32 (**5**): 057302. DOI: 10.1088/1674-1056/ac8e97

Thermoelectric signature of Majorana zero modes in a T-typed double-quantum-dot structure

Cong Wang(王聪) and Xiao-Qi Wang(王晓琦)
Chin. Phys. B, 2023, 32 (**3**): 037304. DOI: 10.1088/1674-1056/ac92d3

Nonlinear Seebeck and Peltier effects in a Majorana nanowire coupled to leads

Feng Chi(迟锋)[1,†], Jia Liu(刘佳)[2], Zhenguo Fu(付振国)[3], Liming Liu(刘黎明)[1], and Zichuan Yi(易子川)[1]

[1] *School of Electronic and Information Engineering, UESTC of China, Zhongshan Institute, Zhongshan* 528400, *China*
[2] *School of Science, Inner Mongolia University of Science and Technology, Baotou* 014010, *China*
[3] *Institute of Applied Physics and Computational Mathematics, Beijing* 100088, *China*

(Received 11 January 2024; revised manuscript received 13 April 2024; accepted manuscript online 17 April 2024)

We theoretically study nonlinear thermoelectric transport through a topological superconductor nanowire hosting Majorana bound states (MBSs) at its two ends, a system named as Majorana nanowire (MNW). We consider that the MNW is coupled to the left and right normal metallic leads subjected to either bias voltage or temperature gradient. We focus our attention on the sign change of nonlinear Seebeck and Peltier coefficients induced by mechanisms related to the MBSs, by which the possible existence of MBSs might be proved. Our results show that for a fixed temperature difference between the two leads, the sign of the nonlinear Seebeck coefficient (thermopower) can be reversed by changing the overlap amplitude between the MBSs or the system equilibrium temperature, which are similar to the cases in linear response regime. By optimizing the MBS–MBS interaction amplitude and system equilibrium temperature, we find that the temperature difference may also induce sign change of the nonlinear thermopower. For zero temperature difference and finite bias voltage, both the sign and magnitude of nonlinear Peltier coefficient can be adjusted by changing the bias voltage or overlap amplitude between the MBSs. In the presence of both bias voltage and temperature difference, we show that the electrical current at zero Fermi level and the states induced by overlap between the MBSs keep unchanged, regardless of the amplitude of temperature difference. We also find that the direction of the heat current driven by bias voltage may be changed by weak temperature difference.

Keywords: quantum dot, nonlinear Seebeck coefficient, Peltier coefficient, Majorana bound states, sign change

PACS: 73.21.La, 72.15.Jf, 73.50.Lw **DOI:** 10.1088/1674-1056/ad3f99

1. Introduction

Majorana bound states (MBSs) are quasiparticle excitations of Majorana fermions, which are of their own antiparticles and thus charge-neutral, as well as zero in energy. They satisfy non-Abelian statistics and are promising in fault-tolerant quantum computation implementations.[1–3] Theoretically, a pair of MBSs were predicted to be realizable at opposite ends of a nanowire on top of a three-dimensional superconductor substrate (Kitaev chain).[4] Inspired by this model, MBSs were further investigated in topological insulators[5] and topological semiconductor-superconductor heterostructures.[6] Signatures might arise from MBSs that were fist observed experimentally by Mourik *et al*. in a semiconductor-superconductor nanowire (Majorana nanowire) composed of indium antimonide (InSb) and niobium titanium nitride (NbTiN).[7] Subsequently, states possessing exotic characteristics of MBSs were found in a semiconductor indium arsenide (InAs) nanowire with a quantum dot (QD) at its one end,[8] phase-controlled Josephson junctions with topological superconductivity,[9,10] a hybrid nanowire consisting of a semiconductor InAs core surrounded by superconductor aluminum (Al) shell,[11] a Kitaev chain sandwiched between two spin-polarized QDs,[12] vortexes in topological superconductors,[13,14] magnetic texture with strong spin–orbit interaction,[15] and some other solid-state platforms.

Along with the preparation of MBSs signature in condensed matter setups, there have been many attempts to detect their existence by an irrefutable experimental evidence. Currently, transport experiments offer a relatively simple way to detect MBSs signatures via the phenomenon of zero-bias anomaly (ZBA) emerging in the electrical conductance due to the exotic zero-energy character of MBSs.[7,8,16] To avoid uncertainty of the ZBA unique to the existence of MBSs, it often requires to perform additional analysis to distinguish MBSs from possibilities of the Kondo effect[17–20] or the partially separated Andreev bound states.[21–25] Other mechanisms that can demonstrate the existence of MBS were also proposed, including spin selective Andreev reflection,[13] fractional and planar Josephson effects,[9,10,26] quantum interference effects in in ring- or T-shaped QDs-based systems,[27–31] etc.

It was shown previously that the MBSs at vortex cores of a two-dimensional topological superconductor with broken time-reversal symmetry can induce a magneto-thermoelectric (Ettingshausen) effect between opposite sides of the edge

[†]Corresponding author. E-mail: chifeng@semi.ac.cn

© 2024 Chinese Physical Society and IOP Publishing Ltd

states.[32] This is due to the fact that the flow of vortex carrying MBSs induces a temperature gradient between the two sides of the topological superconductor, i.e., a phenomenon that could be viewed as an strong evidence of MBSs signature. Further study proved that a nonvanishing thermopower of reasonable magnitude between a conducting lead and a superconductor can be applied to infer the information of MBSs.[33] The thermopower, which is a central quantity in thermoelectric effects, measures the generated bias voltage in response to a temperature difference applied across a system under the condition of zero current. To break the particle–hole symmetry of MBSs, a QD with gate-tunable energy levels was proposed to be inserted between a normal lead and a superconductor possibly hosting MBSs.[34] The emerged thermopower in this setup relies on the coupling strength between the QD and MBSs, and thus information of the MBSs is extractable.[34] If a nanowire hosting signature of MBSs is side-coupled to a QD sandwiched between two leads, the sign of the thermopwer can be efficiently reversed by adjusting the overlap amplitude between the MBSs, QD-MBSs coupling strength, as well as the system equilibrium temperature.[35–37] This is of particular interesting and useful in the detection of possible existence of MBSs.

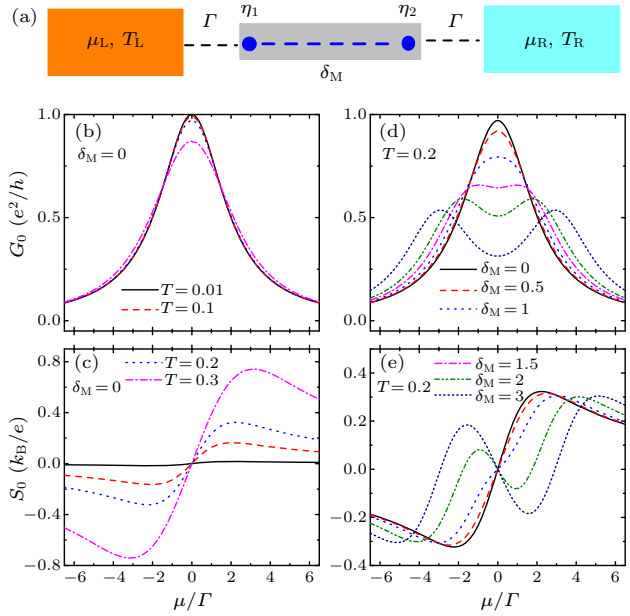


Fig. 1. (a) Schematic plot of the topological superconductor nanowire hosting MBSs, which are denoted individually by η_1 and η_2. The MBSs couple to the left and right normal metal leads with equal strength of Γ. The two leads are held at different temperatures of T_L and T_R, from which the thermoelectric effect arises. The chemical potentials of the leads are presented by μ_α, and δ_M stands for overlap amplitude between the MBSs. [(b), (c)] Individually for the linear conductance G_0 and linear thermopower S_0 as functions of chemical potential of the leads $\mu = \mu_L = \mu_R$ at different values of system temperature $T = T_L = T_R$ with $\delta_M = 0$. [(d), (e)] Individually for G_0 and S_0 with δ_M varying and $T = 0.2$ fixed.

In the above-mentioned work concerning thermoelectric effect mediated by MBSs, the magnitude of bias voltage and temperature difference between two terminals of the system are infinitesimal (linear response regime). Beyond linear response, i.e., in the presence of finite bias voltage and/or temperature difference, the electric and heat currents induced by the applied bias voltage will interfere with those excited by the temperature difference via adjusting the system's parameters, leading to a highly nontrivial thermoelectric effect.[38–44] Recently, nonequilibrium noise due to the fluctuation of electric current under the nonlinear condition was proposed to demonstrate the existence of MBSs in a nanowire side-coupled to a QD connected to leads.[45–47] In the present manuscript, we study nonlinear thermoelectric transport through an MNW sandwiched between the left and right normal mental leads (N-MNW-N). The two leads are biased by a voltage and held at different temperatures as shown in Fig. 1(a). It should be noted that Seebeck effect in the linear response regime has been studied previously in this model.[35,48,49] They found that the thermopower remains to be zero when the leads' chemical potential is aligned to the zero-energy state of the MBSs due to its inherent particle-hole symmetry. Apart from this point, both the magnitude and sign of the thermopower depends on the direct overlap amplitude of the MBSs. In the nonlinear response regime, we find that the sign of the nonlinear thermopower can be reversed by changing temperature difference between the two leads in addition to the MBS–MBS coupling amplitude and the system equilibrium temperature. Under finite bias voltage and zero temperature difference, one can adjust the nonlinear Peltier coefficient by either the bias voltage or overlap amplitude between the MBSs. In the presence of both bias voltage and temperature difference, the direction of the heat current may be reversed by changing the MBS–MBS coupling amplitude, which can be used for cooling or heating the MNW.

2. Model and method

In the low-energy regime, the effective Hamiltonian of the N-MNW-N system can be written as[48–50]

$$H = \sum_{k,\beta=\mathrm{L,R}} \varepsilon_{k\beta} c^\dagger_{k\beta} c_{k\beta} + \frac{\mathrm{i}}{2}\varepsilon_M \gamma_1 \gamma_2 + \sum_k (V_L \gamma_1 c_{k\mathrm{L}} + V_R c_{k\mathrm{R}} \gamma_2 + \mathrm{H.c.}), \quad (1)$$

where the first term on the right-hand side of Eq. (1) is for the normal metal leads with continuous energy $\varepsilon_{k\beta}$ and creation (annihilation) operator $c^\dagger_{k\beta}$ ($c_{k\beta}$). The second and third terms on the right-hand side of Eq. (1) represent the MBSs at the ends of the MNW and their interaction to the leads.[49,50] The operator $\gamma_{1(2)}$ satisfies $\gamma_{1(2)} = \gamma^\dagger_{1(2)}$, $\gamma^2_{1(2)} = 1$ and the anti-communication relationship of $\{\gamma_i, \gamma_j\} = 2\delta_{ij}$. The quantity δ_M is the direct hybridization amplitude between the MBSs, and V_β stands for hybridization strength between the MBSs and the β-th lead. We calculate the electrical and heat currents flowing through lead β by the nonequilibrium Green's

function technique,[48,49]

$$I_\beta = \frac{e}{h}\int \mathrm{d}\varepsilon \mathcal{T}(\varepsilon)[f_{\mathrm{L}}(\varepsilon) - f_{\mathrm{R}}(\varepsilon)], \tag{2}$$

$$J_\beta = \frac{e}{h}\int \mathrm{d}\varepsilon(\varepsilon - \mu_\beta)\mathcal{T}(\varepsilon)[f_{\mathrm{L}}(\varepsilon) - f_{\mathrm{R}}(\varepsilon)], \tag{3}$$

where $f_\beta(\varepsilon) = 1/\{\exp[(\varepsilon-\mu_\beta)/(k_{\mathrm{B}}T_\beta)]+1\}$ is the Fermi-Dirac distribution function with k_{B} being the Boltzmann constant, T_β and μ_β are temperature and Fermi energy in the β-th lead, respectively. Due to the current conservation, the relationship $I_{\mathrm{L}} = -I_{\mathrm{R}} = I$ is satisfied. The transmission coefficient $\mathcal{T}(\varepsilon)$ in Eqs. (2) and (3) is calculated in terms of the retarded/advanced Green's function of the MBSs $G_\gamma^{\mathrm{r/a}}(\varepsilon)$. By employing the equation of motion method, one obtains the matrix expression of $G_\gamma^{\mathrm{r/a}}(\varepsilon)$ as follows:[48–50]

$$\hat{G}_\gamma^{\mathrm{r/a}}(\varepsilon) = \frac{2}{\varepsilon + \delta_{\mathrm{M}}\hat{\sigma}_y - 2\hat{\Sigma}_0^{\mathrm{r/a}}}, \tag{4}$$

in which $\hat{\sigma}_y$ is the usual Pauli matrix of the y-component, $\hat{\Sigma}_0^{\mathrm{r/a}} = \mathrm{diag}(-\mathrm{i}\Gamma_{\mathrm{L}}/2, -\mathrm{i}\Gamma_{\mathrm{R}}/2)$ the self-energy due to the presence of the leads. The line-width function in the above expression is given by $\Gamma_\beta = 2\pi|V_\beta|^2\sum_k \delta(\varepsilon - \varepsilon_{k\beta})$. In this manuscript, we consider symmetrical coupling between the MNW and the left and right leads, and set $\Gamma = \Gamma_{\mathrm{L}} = \Gamma_{\mathrm{R}}$. The transmission coefficient in Eqs. (2) and (3) is then given by $\mathcal{T}(\varepsilon) = \Gamma(\mathrm{G}^{\mathrm{r}}_{\gamma;11} + \mathrm{G}^{\mathrm{r}}_{\gamma;22})/2$, whose explicit expression is[48–50]

$$\mathcal{T}(\varepsilon) = \frac{4\Gamma^2(\varepsilon^2 + \delta_{\mathrm{M}}^2 + 4\Gamma^2)}{(\varepsilon^2+4\Gamma^2)^2 + \delta_{\mathrm{M}}^2[\delta_{\mathrm{M}}^2 - 2(\varepsilon^2 - 4\Gamma^2)]}. \tag{5}$$

The nonlinear Seebeck and Peltier coefficients are numerically calculated as $S_{\mathrm{n}} = -\Delta V/\theta$ under the condition of zero electrical current $I_{\mathrm{L}} = -I_{\mathrm{R}} = I = 0$, and $\Pi_{\mathrm{n}} = J_{\mathrm{L}}/I_{\mathrm{L}}$ in the absence of temperature difference. Here $\theta = T_{\mathrm{L}} - T_{\mathrm{R}}$ is the temperature difference between the left and right leads. In what follows, we set $T_{\mathrm{L}} = T + \theta$ and $T_{\mathrm{R}} = T$, with T being the system equilibrium temperature. The chemical potential of the left lead is set to be $\mu_{\mathrm{L}} = \mu + eV$, where μ is the chemical potential in equilibrium state, and V is the bias voltage applied across the system. The chemical potential of the right lead is fixed at $\mu_{\mathrm{R}} = \mu$.

3. Numerical results

In the following numerical calculations, the line-width function $\Gamma \equiv 1$ is chosen as the energy unit. We first summarize briefly behaviors of electrical conductance $G_0(\mu)$ and thermopower $S_0(\mu)$ in the linear response regime (here we choose infinitely small $\theta = eV = 10^{-4}$). We have checked that the following results are the same to those obtained from linear-response formulae ($eV = \theta = 0$) such as in Refs. [49, 50]. It is well known that in this regime, the Peltier coefficient Π_0 is related to the thermopower by $\Pi_0 = TS_0$ (Kelvin relation).[39,40] When the MBSs are decoupled from each other $\delta_{\mathrm{M}} = 0$, the peak in G_0 is widened and lowered with increasing equilibrium temperature T as more electrons in the leads are excited to higher energy states, as shown in Fig. 1(b). The linear thermopower S_0 in Fig. 1(c) is antisymmetrical with respective to the state of $\mu = 0$, and is enhanced significantly by increased temperature T. It has two maximum absolute values when the Fermi energy in the leads is $|\mu| \approx 2\Gamma$. In the presence of MBS–MBS hybridization ($\delta_{\mathrm{M}} \neq 0$) as shown in Fig. 1(d), the central peak in G_0 is lowered and split when $\delta_{\mathrm{M}} > \Gamma$[49,50] because new states are induced. As for S_0 in Fig. 1(e), its lineshape resembles that of $\delta_{\mathrm{M}} = 0$, and then changes its sign when $\delta_{\mathrm{M}} > \Gamma$. These results are in agreement with those found in previous work.[49]

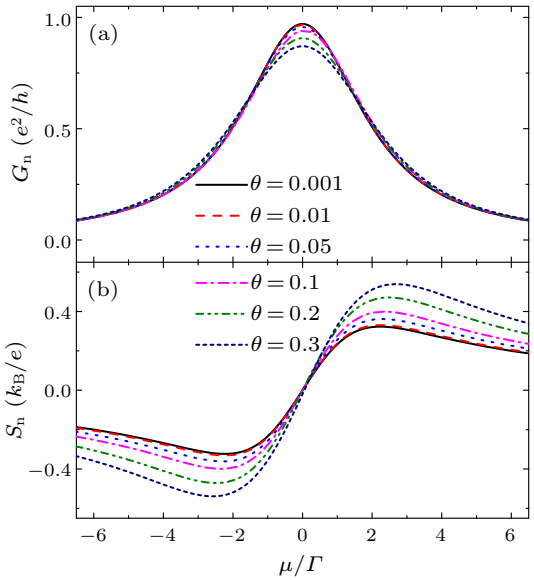


Fig. 2. Differential conductance G_{n} in (a) and nonlinear thermopower S_{n} in (b) as functions of μ for different values of the temperature difference between the leads, $\theta = T_{\mathrm{L}} - T_{\mathrm{R}}$. Other parameters are $\delta_{\mathrm{M}} = 0$, equilibrium temperature $T = 0.2$, and an infinitesimal bias voltage $eV = 10^{-7}$. For sufficiently small $\theta = 0.001$, G_{n} and S_{n} correspond to their linear counterparts.

We then study the nonlinear thermoelectric effects, focusing our attention on the sign change of the nonlinear thermopower S_{n} and Peltier coefficient Π_{n}, and consider three different cases: (1) isoelectric case ($eV = 0, \theta \neq 0$) to study the nonlinear thermopower S_{n}; (2) isothermal case ($\theta = 0, eV \neq 0$) to examine the nonlinear Peltier coefficient Π_{n}; and (3) finite both θ and eV to investigate the thermocurrent. Figures 2(a) and 2(b) show the nonlinear electrical conductance $G_{\mathrm{n}} = \mathrm{d}I/\mathrm{d}V$ and thermopower S_{n} for different θ under the conditions of zero δ_{M} and infinitesimal bias voltage. When the temperature difference is sufficiently small ($\theta = 10^{-3}$), the nonlinear conductance in Fig. 2(a) resembles its linear counterpart in Fig. 1(b). With increasing θ, the peak in G_{n} is lowered and broadened as more electrons are excited above the Fermi level in the left hotter lead. The behavior of the nonlinear thermopower in Fig. 2(b) also resembles that of its linear counterpart in Fig. 1(c),[48,49] with $S_{\mathrm{n}}(\mu = 0) \equiv 0$. This is due

to the fact that the difference between the Fermi functions in the left and right leads $f_{\rm L}(\varepsilon)-f_{\rm R}(\varepsilon)$ is an odd function of μ, and then the electrical current I is zero at $\mu=0$ due to the particle-hole symmetry nature of the MBSs. When the left lead is heated ($\theta>0$), more electrons are excited above the chemical potential as indicated earlier. These electrons will carry more energy from the left lead to the right one, leading to larger thermopower as shown in Fig. 1(c).

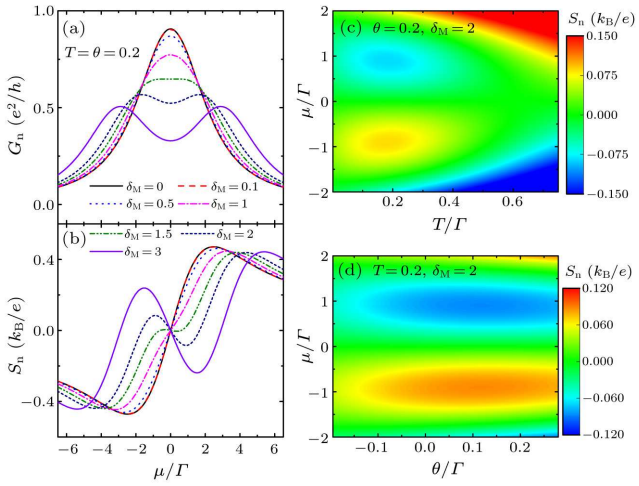


Fig. 3. (a) Differential conductance $G_{\rm n}$ and (b) nonlinear thermopower $S_{\rm n}$ varying with respective to μ for different values of $\delta_{\rm M}$ and fixed $T=\theta=0.2$. [(c), (d)] Contour plots of $S_{\rm n}$ as a function of (μ, T) and (μ, θ), respectively. The bias voltage is set to be $eV\approx 0$. [(b), (c)] Sign of $S_{\rm n}$ is reversible by changing the values of $\delta_{\rm M}$ and system equilibrium T.

We then show the impacts of MBS–MBS hybridization $\delta_{\rm M}$ on $G_{\rm n}$ and $S_{\rm n}$ in Fig. 3 under finite θ and infinitesimal bias voltage. When the MBSs on opposite ends of the MNW are overlapped ($\delta_{\rm M}\neq 0$), the central peak in $G_{\rm n}$ is broadened and lowered as shown in Fig. 3(a). If the amplitude of $\delta_{\rm M}$ exceeds the coupling strength between the leads and the MNW ($\delta_{\rm M}>\Gamma$), the central peak is split into two peaks positioned individually at about $\mu\approx\delta_{\rm M}$. These behaviors of $G_{\rm n}$ are also similar to those of its linear counterpart,[49] but with reduced amplitude as a result of the increased temperature in the left lead. The nonlinear thermopower $S_{\rm n}$ in Fig. 3(b) remains to be zero at the point of $\mu=0$, and is antisymmetrical with respective to this point regardless of the value of $\delta_{\rm M}$. There is an obvious sign change in $S_{\rm n}$ under the conditions of $\delta_{\rm M}>\Gamma$ and $\mu\leq|\delta_{\rm M}|$, which has also been found in previous work.[49] Here we prove that this phenomenon survives under finite temperature gradient across the system. To further explore the possibility of the sign change of $S_{\rm n}$, we show counter plots of $S_{\rm n}$ as a function of the chemical potential μ and the equilibrium temperature T in Fig. 3(c) and temperature difference θ in Fig. 3(d). For the chosen parameters, $S_{\rm n}$ in Fig. 3(c) has two peaks of opposite signs positioned individually around $\mu=\pm\Gamma$ as $T\sim\theta$. Figure 3(c) indicates two ways of reversing the sign of $S_{\rm n}$: one is to fix the temperature T and change the chemical potential μ, which is the case shown in Fig. 3(b); the other is to fix the chemical potential such as at $\mu=\pm\Gamma$ and adjust the temperature T. Here we emphasize that the sign change of linear thermopower induced by adjusting equilibrium temperature was previously found in system composed of a QD (regular fermions) coupled to leads.[51] Quite different from the cases in QD-based systems, the sign change of nonlinear thermopower in the present MNW mainly arises from the states arisen in low temperature regime. The reason is that the MBSs induce new molecular states near the chemical potential, which are absent in QD-based systems. The resonances in $S_{\rm n}$ around $\mu\sim\Gamma$ are robust against the change of θ as shown in Fig. 3(d). With the change of θ from negative to positive values, both the width and height of the peaks in $S_{\rm n}$ keep almost unchanged. This enables the observation of sign change of $S_{\rm n}$ with respective to the chemical potential μ or system temperature T.

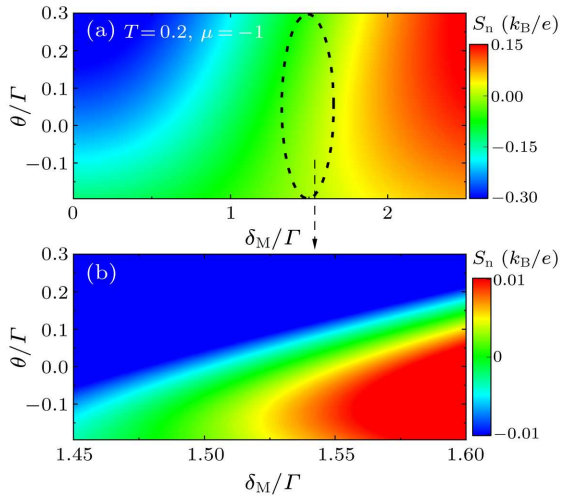


Fig. 4. (a) The $S_{\rm n}$ as a function of μ and θ for the indicated parameter. (b) The blowup of (a) to show that the sign of $S_{\rm n}$ can be reversed by properly changing θ and $\delta_{\rm M}$ at a fixed μ.

Figure 3(d) shows that $S_{\rm n}$ does not change its sign by varying θ for the given values of $\delta_{\rm M}=2$ and $T=0.2$. Since both $\delta_{\rm M}$ and T can induce sign change of $S_{\rm n}$, we then believe that $\delta_{\rm M}$ has a transition value at which the sign of $S_{\rm n}$ is reversible by varying θ. We therefore study the behavior of $S_{\rm n}$ as a function of θ and $\delta_{\rm M}$ in Fig. 4 with fixed $\mu=-1$ and $T=0.2$. We find from Fig. 4(a) that the value of $S_{\rm n}$ changes from negative to positive or vice versa by increasing $\delta_{\rm M}$ at any θ. Moreover, the magnitude of $S_{\rm n}$ is enhanced nonlinearly by increasing θ for fixed $\delta_{\rm M}$, which indicates that the sign of $S_{\rm n}$ may be reversed by changing θ for a certain value of $\delta_{\rm M}$. This supposition is confirmed by Fig. 4(b), in which $S_{\rm n}$ changes its sign by the variation of θ around $\delta_{\rm M}=1.5$. We emphasize that this phenomenon has never been reported before, and attribute it to the combined functions of $\delta_{\rm M}$ and temperature T on the sign of $S_{\rm n}$. Moreover, the nonlinear thermopower $S_{\rm n}$ may change its sign at very weak θ for $\delta_{\rm M}\sim 1.5$.

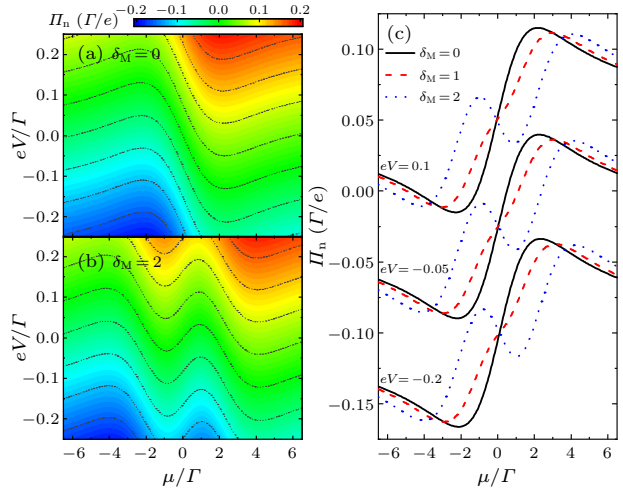


Fig. 5. Counter plot of the Peltier coefficient Π_n versus bias voltage eV and chemical potential μ for $\delta_M = 0$ in (a) and $\delta_M = 2$ in (b). (c) Π_n as a function of μ at three values of eV, with $\delta_M = 0, 1, 2$. The equilibrium temperature and temperature difference are set to be $T = \theta = 0.2$.

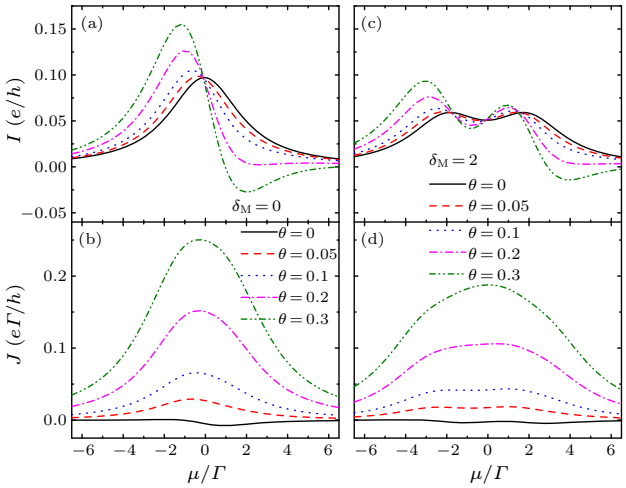


Fig. 6. [(a), (c)] Thermocurrent $I(eV, \theta)$ and [(b), (d)] heat current $J(eV, \theta)$ versus μ at different values of temperature difference θ. The bias voltage and system equilibrium temperature are set to be $eV = 0.1$ and $T = 0.2$, respectively.

We next study in Fig. 5 the behaviors of nonlinear Peltier coefficient Π_n under the conditions of finite bias voltage ($eV \neq 0$) and zero temperature difference ($\theta = 0$). When the two modes of MBSs are decoupled from each other ($\delta_M = 0$), Π_n is characterized by two resonances positioned individually in the negative and positive Fermi energy regimes, as shown in Fig. 5(a). With increasing (decreasing) bias voltage, the lineshape of Π_n versus μ remains unchanged and is shifted toward positive (negative) regime. The reason is that with increasing bias voltage, the electronic transport window is enlarged and enables more electrons to tunneling through the device, resulting in larger current. Here we find that the sign of the nonlinear Peltier coefficient is reversible by changing the direction of the bias voltage due to the property of the current. When the MBSs are overlapped ($\delta_M \neq 0$) as shown in Fig. 5(b), two new resonances emerge at two sides of $\mu = 0$, which is similar to the case in the nonlinear thermopower as shown in Fig. 3(b). Now variation of Π_n with respective to the bias voltage resembles to that of Fig. 5(a). In Fig. 5(c), we show impacts of different values of both bias voltage eV and inter-MBS coupling δ_M on Π_n. It confirms the results in Figs. 5(a) and 5(b), and indicates that both the sign and the magnitude of Π_n can be efficiently adjusted by tuning either bias voltage or overlap amplitude between the MBSs.

In Fig. 6 we study the electrical current I and thermocurrent J varying with respective to the chemical potential μ in the presence of finite both bias voltage and temperature difference. For $\delta_M = 0$, the electrical current I is positive ($eV = 0.1$) and develops a broad peak at $\mu = 0$ in the absence of temperature difference ($\theta = 0$) as indicated by the black solid line in Fig. 6(a). With increasing θ, the value of $I(\mu = 0)$ remains unchanged due to the property of the transmission coefficient $\mathcal{T}(\varepsilon)$. Moreover, the electrical current I becomes antisymmetrical with respective to $\mu = 0$. The peak in I moves toward negative μ regime with enhanced value, and the value of I is suppressed in the regime of $\mu > 0$. For sufficiently large θ, a negative dip emerges. The heat current J is rather weak and antisymmetrical to $\mu = 0$ as is shown by the black solid line in Fig. 6(b). In the presence of finite θ, it develops a broad peak centered at $\mu = -eV$ and is monotonously enhanced by increasing θ due to the fact that more electrons are excited into the transport window. When the MBSs are overlapped ($\delta_M = 2$), the magnitudes of both electrical and heat currents are reduced as shown in Figs. 6(c) and 6(d). This is because the magnitude of transmission coefficient or the conductance in Fig. 3(a) is weakened for nonzero δ_M. Since the central peak in the conductance is split into $\mu = \pm\delta_M$ when $\delta_M > \Gamma$, the electrical current in Fig. 6(c) keeps unchanged at these two points regardless of the value of θ, which is similar to the case for $\mu = 0$. As shown in Fig. 6(d), the peak in heat current becomes flatter as is compared to the case of $\delta_M = 0$ because more higher energy electrons participate in the transport processes when the left lead is heated ($\theta > 0$).

4. Conclusion

In summary, nonlinear thermoelectric transport through a Majorana nanowire coupled to the left and right normal metallic leads is studied within the nonequilibrium Green's function technique. We find that the sign of the nonlinear thermopower is reversible by adjusting the value of direct MBS–MBS coupling strength or the system equilibrium temperature. By properly choosing the overlap amplitude between the MBSs and system equilibrium temperature, the sign of the nonlinear thermopower can also be changed by varying the temperature difference. In the presence of bias voltage, both the sign and magnitude of nonlinear Peltier coefficient can be adjusted by changing the magnitude of bias voltage or MBS–MBS coupling strength. Excited by both bias voltage and temperature difference, the electrical current through the

states originated from overlap between the MBSs keeps unchanged regardless of the strength of temperature difference when the leads' chemical potential is in resonance with the energy of MBSs. Now the direction of the heat current driven by bias voltage may be changed at weak temperature difference.

Acknowledgments

Project supported by the National Natural Science Foundation of China (Grant No. 12264037), the Innovation Team of Colleges and Universities in Guangdong Province (Grant No. 2021KCXTD040), Guangdong Province Education Department (Grant No. 2023KTSCX174), the Key Laboratory of Guangdong Higher Education Institutes (Grant No. 2023KSYS011), and Science and Technology Bureau of Zhongshan (Grant No. 2023B2035).

References

[1] Nayak C, Simon S H, Stern A, *et al.* 2008 *Rev. Mod. Phys.* **80** 1083
[2] Alicea J, Oreg Y, Refael G, *et al.* 2011 *Nat. Phys.* **7** 412
[3] Sau J D, Lutchyn R M, Tewari S and Sarma S D 2010 *Phys. Rev. Lett.* **104** 040502
[4] Kitaev A Yu 2001 *Phys. Usp.* **44** 131
[5] Fu L and Kane C L 2008 *Phys. Rev. Lett.* **100** 096407
[6] Lutchyn R M, Sau J D and Sarma S D 2010 *Phys. Rev. Lett.* **105** 077001
[7] Mourik V, Zuo K, Frolov S M, *et al.* 2012 *Science* **336** 1003
[8] Deng M T, Vaitiekenas S, Hansen E B, *et al.* 2016 *Science* **354** 1557
[9] Fornieri A, Whiticar A M, Setiawan F, *et al.* 2019 *Nature* **569** 89
[10] Ren H, Pientka F, Hart S, *et al.* 2019 *Nature* **569** 93
[11] Vattekenas S, Winkler G W, van Heck B, *et al.* 2020 *Science* **367** 6485
[12] Dvir T, Wang G Z, van Loo N, *et al.* 2023 *Nature* **614** 445
[13] Sun H H, Zhang K W, Hu L H, *et al.* 2016 *Phys. Rev. Lett.* **116** 257003
[14] Li M, Li G, Cao L, *et al.* 2022 *Nature* **606** 890
[15] Gungordu U and Kovalev A A 2022 *J. Appl. Phys.* **132** 041101
[16] Zhang G, Li C, Li G, *et al.* 2023 *Phys. Rev. B* **107** 195413
[17] Wang R, Su W, Zhu J X, *et al.* 2019 *Phys. Rev. Lett.* **122** 087001
[18] Weymann I, Wojcik K P and Majek P 2020 *Phys. Rev. B* **101** 235404
[19] Majek P and Weymann I 2022 *J. Magn. Magn. Mater.* **549** 168935
[20] Lee S, Choi Y S, Do S H, *et al.* 2023 *Nat. Commun.* **14** 7405
[21] Wang S X, Li Y X and Liu J J 2016 *Chin. Phys. B* **25** 037304
[22] Feng G H and Zhang H H 2022 *Phys. Rev. B* **105** 035148
[23] Ricco L S, de Souza M, Figueira M S, *et al.* 2019 *Phys. Rev. B* **99** 155159
[24] Prada E, San-Jose P, de Moor M W A, *et al.* 2020 *Nat. Rev. Phys.* **2** 575
[25] Zhang S, Wang Z C, Pan D, *et al.* 2022 *Phys. Rev. Lett.* **128** 076803
[26] Fu L and Kane C L 2009 *Phys. Rev. B* **79** 161408
[27] Li Y X and Bai Z M 2013 *J. Appl. Phys.* **114** 033703
[28] Wang N, Lv S H and Li Y X 2014 *J. Appl. Phys.* **115** 083706
[29] Gong W J, Zhang S F, Li Z C, *et al.* 2014 *Phys. Rev. B* **89** 245413
[30] Xia J J, Duan S Q and Zhang W 2015 *Nanoscale Res. Lett.* **10** 223
[31] Jiang C and Zheng Y S 2015 *Solid State Commun.* **212** 14
[32] Hou Y C, Shtengel K, Refael G and Goldbar P M 2012 *New J. Phys.* **14** 105005
[33] Hou Y C, Shtengel K and Refael G 2013 *Phys. Rev. B* **88** 075304
[34] Leijinse M 2014 *New. J. Phys.* **16** 015029
[35] López R, Lee M, Serra L and Lim J S 2014 *Phys. Rev. B* **89** 205418
[36] Hong L, Chi F, Fu Z G, *et al.* 2020 *J. Appl. Phys.* **127** 124302
[37] Chi F, Fu Z G, Liu J, *et al.* 2020 *Nanoscale Res. Lett.* **15** 79
[38] David S and Rosa R 2013 *Phys. Rev. Lett.* **110** 026804
[39] Rosa L and Sanchez D 2013 *Phys. Rev. B* **88** 045129
[40] Zhen Y, Can Z, Jiao K Y, *et al.* 2021 *Acta Phys. Sin.* **70** 108402 (in Chinese)
[41] Wang Y D, Zhu Z G and Su G 2022 *Phys. Rev. B* **106** 035148
[42] Manaparambil A and Weymann I 2023 *Phys. Rev. B* **107** 085404
[43] Daroca D P, Roura-Bas P and Aligia A A 2023 *Phys. Rev. B* **108** 155117
[44] Hwang S Y, Sothmann B and Sánchez D 2023 *Phys. Rev. B* **107** 245412
[45] Smirnov S 2015 *Phys. Rev. B* **92** 195312
[46] Smirnov S 2017 *New J. Phys.* **19** 063020
[47] Smirnov S 2018 *Phys. Rev. B* **97** 165434
[48] Lim J S, Lopez R and Serra L 2012 *New J. Phys.* **14** 083020
[49] Ramos-Andrade J P, Avalos-Ovando O, Orellana P A and Ulloa S E 2016 *Phys. Rev. B* **94** 155436
[50] Flensberg K 2010 *Phys. Rev. B* **82** 180516
[51] Dubi Y and Ventra M D 2013 *Rev. Mod. Phys.* **83** 131